AFCRL-63-62

INVESTIGATION OF CARRIER INJECTION ELECTROLUMINESCENCE

BY

A. G. FISCHER
W. H. FONGER
A. S. MASON

RADIO CORPORATION OF AMERICA
RCA LABORATORIES
PRINCETON, NEW JERSEY

SEMIANNUAL SCIENTIFIC REPORT NO. 3
FOR THE PERIOD
JULY 15, 1962 TO JANUARY 15, 1963

CONTRACT NO. AF19(604)8018
PROJECT NO. 4608, TASK NO. 460804

FEBRUARY 15, 1963

PREPARED FOR
ELECTRONIC RESEARCH DIRECTORATE
AIR FORCE CAMBRIDGE RESEARCH LABORATORIES
OFFICE OF AEROSPACE RESEARCH
UNITED STATES AIR FORCE
BEDFORD, MASSACHUSETTS

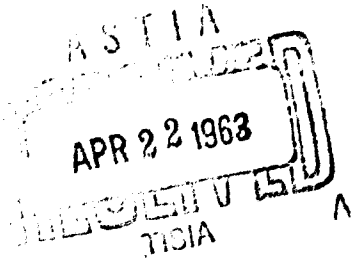

ABSTRACT

The following advances in the growth of crystals of II-VI compounds (ZnSe and ZnTe) and in preparing electroluminescent junctions are related: A magnetic Czochralski puller for temperatures where magnets normally lose their susceptibility has been constructed. Experiences with the epitaxial growth of ZnSe and ZnTe are described. N-type ZnSe crystals exhibit light absorption due to free carriers. Electroluminescent emission at non-ohmic contacts is due to impact-ionization excitation. The new concept of tunnel-injection electroluminescence has been reduced to practice; light emission from CdS layers has been obtained. A new effect, electrical modulation of photoluminescence in CdS, has been discovered. The compounds AlP and BP are apparently not miscible. The value for the lattice constant of AlP has been corrected. Injection electroluminescence was observed in boron phosphide crystals.

The methods for evaporation of ZnSe films on hot substrates were improved, and the light scattering and luminescent properties of such films were studied.

TABLE OF CONTENTS

LIST OF ILLUSTRATIONS

INTRODUCTION

This is the sixth report prepared under this contract. In the previous reports

Scientific Report No. 1	AFCRL 360
Scientific Report No. 2	AFCRL 721
Scientific Report No. 3	AFCRL 979
Semiannual Scientific Report No. 1	AFCRL 62-142
Semiannual Scientific Report No. 2	AFCRL 62-588

we described our work on the following major topics:

- Development of the technology of melt-growth of II-VI compounds
- Properties of crystals prepared from the melt
- Preparation and properties of thin films and electroluminescent junctions
- Investigation of the mechanism of AC-electroluminescence in embedded ZnS powder
- Exploration of wide-gap III-V compounds for electroluminescent purposes

In this report period, this work has been continued, with the final objective of obtaining efficient injection electroluminescence in the visible spectral range at or above room temperature. Our work on the electroluminescence of ZnS powder has been brought to a conclusion (see Semiannual Scientific Report No. 2) and has been discontinued.

I. PREPARATION OF II-VI CRYSTALS

Crystals of the II-VI group, such as ZnS, CdS, ZnSe, ZnO, are the most efficient photoluminescent materials for emission in the visible spectral range at room temperature. They are direct-bandgap compounds. To make single crystals of these materials available for injection electroluminescence research and other purposes, it is desirable to grow these crystals by methods similar to those used in semiconductor technology.

A. NEW MAGNETIC CZOCHRALSKI APPARATUS FOR VAPOR TEMPERATURES EXCEEDING THE CURIE TEMPERATURE OF MAGNETS*

In the last report (AFCRL 62-588, p. 80) we described a new principle which permits magnetic pulling under the clean conditions found in sealed ampoules, despite the fact that the vapor temperatures required for II-VI compounds exceed the temperature at which steel loses its magnetism. This idea led to the construction of the device shown in Fig. 1 which is now ready for use.

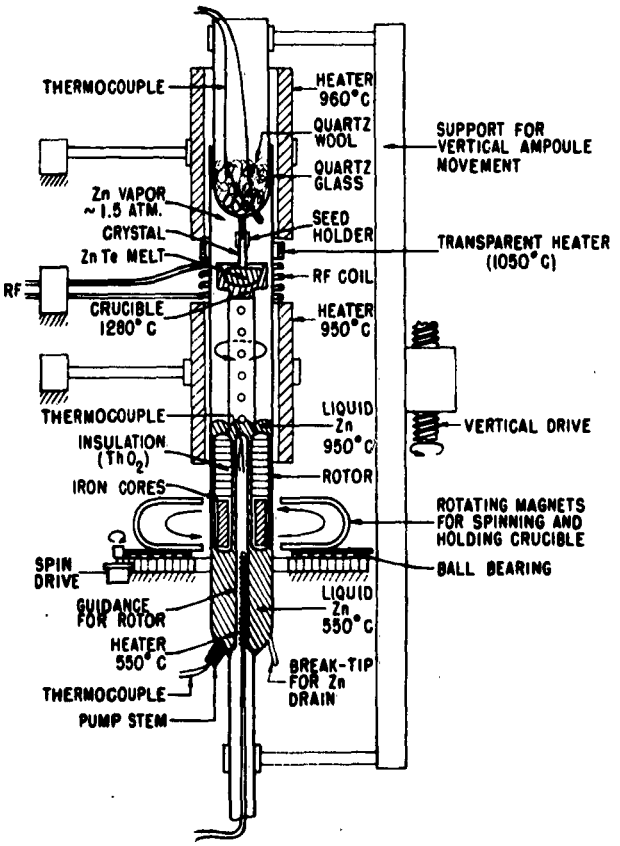

Fig. 1. Magnetic Czochralski apparatus for II-VI compounds, where the vapor temperatures exceed the Curie point of magnets.

*Work done by A. G. Fischer

The crucible which contains the melt is spun and withdrawn by rotating magnets which are immersed in a liquid zinc bath. The ampoule, with the crystal seed firmly attached to it, is held in place. The zinc bath is heated to the temperature (~ 1000°C) which corresponds to the desired vapor pressure (1-3 atm.) only at its top surface. The lower volume, in which the magnets rotate, is held at about 500°C where the magnetic susceptibility is still strong. Operational experiences with this system will be related in the next report. A promising innovation which is also being tested at present is a new differential manometer (Fig. 2) which permits equilibration of internal and external pressure in a growth ampoule to prevent explosions and implosions.

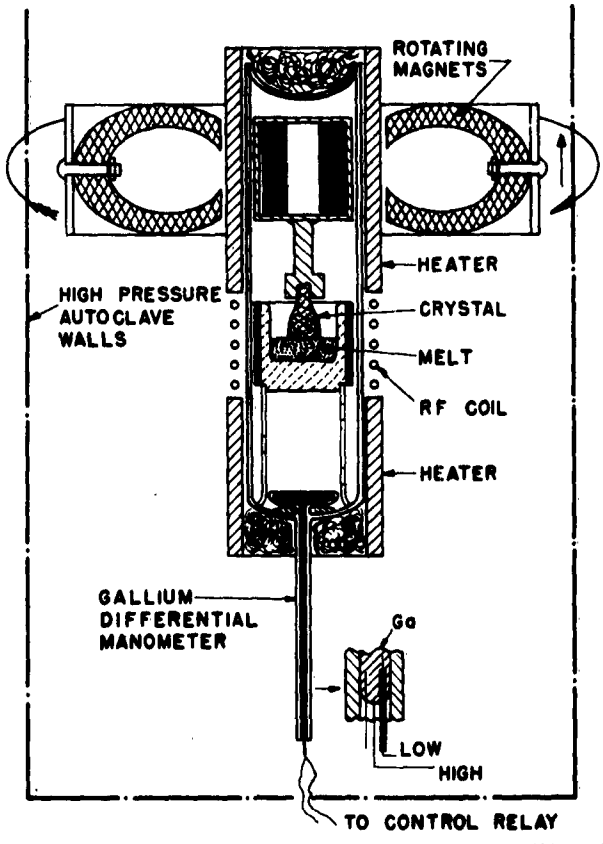

Fig. 2. Differential quartz manometer to permit equilibration of external and internal pressure.

B. BRIDGMAN GROWTH OF ZnTe*

The resistance-heated Bridgman apparatus for ZnTe described in the previous report (p. 79) was used in several runs. The maximum grain size achieved to date is 1 × 3 × 5 mm. Attempts to improve the crystallinity by varying the furnace gradient have not been rewarding. All successful

*Work done by A. S. Mason

runs to date have been made with about 1 atm. of zinc pressure. A run with 1 atm. of tellurium pressure resulted in sublimation of the entire charge of ZnTe. Both quartz and graphite boats have been used successfully. Although an unpredictable darkening of the crystals sometimes occurs with graphite, grain size is frequently larger than with quartz. Strain induced by sticking to the quartz probably causes the poorer crystallinity.

C. VAPOR PHASE GROWTH OF ZnSe-ZnTe*

As study of p-n junctions in ZnSe is hampered by the difficulty of obtaining conducting p-type regions in ZnSe, and vice versa in ZnTe, studies were initiated of alloying ZnSe with ZnTe in hope of obtaining a material in which junctions can be formed readily. ZnSe and ZnTe form a continuum of solid solutions whose lattice constants follow Vegard's law.[1] In Report No. 2, AFCRL 721 p. 16, we showed that the p-type conductivity of ZnTe can be maintained up to high ZnSe additions.

In the present work, commercial ZnSe and ZnTe were ground together and fired under argon at 1000°C for several hours. The resulting sintered material was used for either conventional sublimation procedures in a flowing gas stream or Czysak- Piper-type moving gradient sublimation.[2] The former technique yielded small crystals whose bandgap varied according to location within the apparatus. These ranged from pure ZnTe to intermediate composition. The Czysak-Piper method resulted in ingots of graduated composition. Sublimation temperatures of 1200°C were used, in an apparatus similar to that of Fig. 20, Scientific Report No. 1 (AFCRL 360).

Neither technique having provided alloyed crystals of a size sufficient for the desired experiments, a different approach was developed.

D. EPITAXIAL GROWTH OF ZnSe-ZnTe*

Since transport methods have proved successful with mixed III-V systems,[3] additional work has been undertaken on the apparatus for epitaxial growth illustrated on p. 87, Scientific Report No. 2 (AFCRL 62-588) with the intent of extending the technique to mixtures of II-VI compounds. Initial work with pure ZnSe has yielded mirror-smooth photoluminescent films on GaAs wafers of (1, 1, 1) orientation. These films have been evaporated in an atmosphere of either H_2, or H_2 passed over iodine at room temperature. Continuous films have, so far, not been grown on Ge wafers, since attack on them causes etch pits which are propagated as pinholes in the films. This attack is probably due to evaporated selenium, since it occurs in either hydrogen or argon atmosphere without the addition of iodine. Thermal etching may be another possibility.

Luminescent films have also been deposited on quartz substrates by these methods.

*Work done by A. S. Mason

Current efforts are directed toward increasing the growth rate in order to make films sufficiently thick to be removed from the substrate. Use of bromine at 0°C as the transport agent has been attempted, but it appears to attack the GaAs excessively.

A workable way of producing thick films would be a suitable alternative to crystal growth in the usual sense. Extension of this work to ZnTe and Zn (Se, Te) mixtures is planned.

E. PROPERTIES OF n-TYPE ZnSe CRYSTALS*

1. Collision-Ionization Electroluminescence

The ZnSe crystals grown from the melt under high zinc pressure by the vertical Bridgman technique are highly n-type, photoluminescent and show impact-ionization EL at negatively biased, non-ohmic (slightly blocking) contacts (p. 69, Semiannual Scientific Report No. 2, AFCRL 62-588).

Recently, Lozykowski in Torun (Poland) reported that he had succeeded in preparing electroluminescent p-n junctions in ZnSe.[4] His allegedly p-type, luminescent crystals were grown in a conventional way by sublimation and had diffused gold and indium contacts. They emitted at forward bias. The crystals were very small so that the origin of the light (cathode or anode) could probably not be distinguished.

In our opinion, which is based on experience collected over the last two years, Lozykowski's crystals cannot have been p-type, but most certainly were n-type. By making a diode wafer structure as shown in Fig. 3a, with a blocking gold contact and a slightly blocking indium contact, one obtains a structure which emits brightly at forward bias (Fig. 4). This can easily mislead to the conclusion that one has made an injecting contact.

With a structure shown in Fig. 3b, however, the origin of the radiation (cathode) is easily discernible, and it is immediately evident that the effect is caused by impact ionization in the high field of a cathodic depletion layer (Fig. 5).

2. Free-Carrier Absorption in n-Type ZnSe

From our Hall-effect measurements (p. 67, Semiannual Scientific Report No. 2, AFCRL 62-588) it can be concluded that the free-carrier concentration in n-type ZnSe grown under zinc pressure is very high, between 10^{18} and 10^{19} per cm^3. According to the well-known Drude-Zener theory of plasma absorption, this should lead to light absorption by free carriers in the near infrared.

*Work done by A. G. Fischer

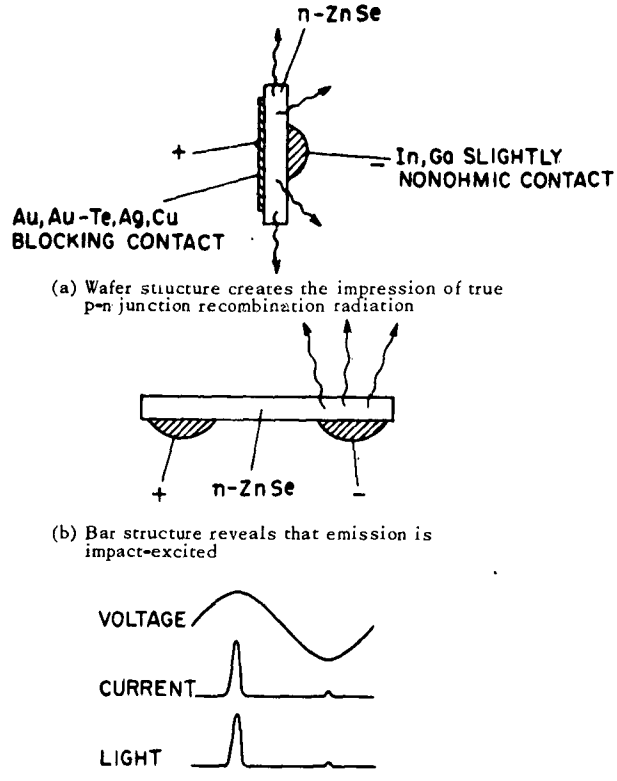

Fig. 3. Construction of ZnSe EL diodes.

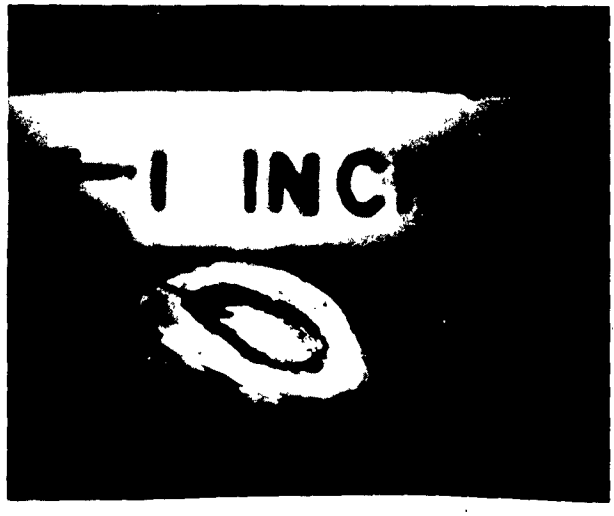

Fig. 4. Photograph of light emission from a ZnSe diode.

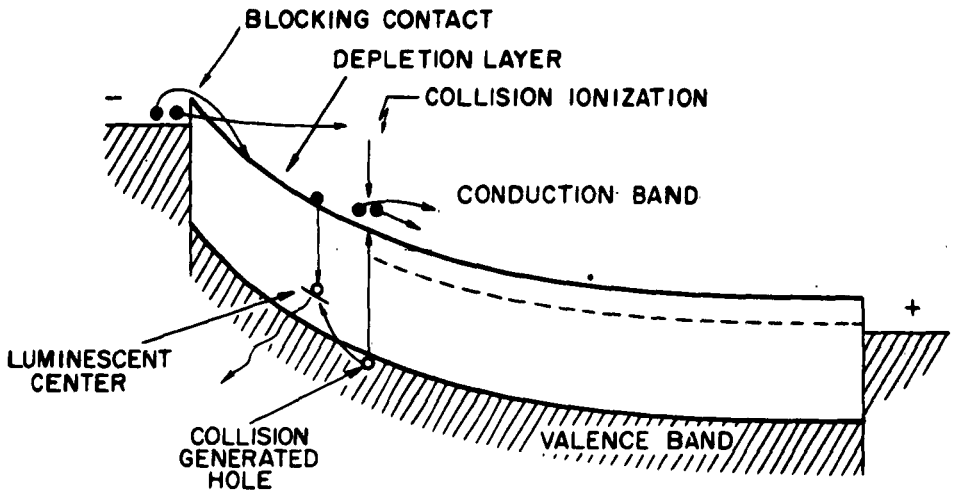

Fig. 5. Illustration of DC-EL impact-ionization mechanism.

Absorption measurements with a Perkin-Elmer Spectrometer showed indeed such an absorption (Fig. 6). The absorption does not follow the λ^2 dependence as postulated by the theory in its simplest form, but deviates from this, having an average slope which is steeper, with several bumps in it. We have not attempted as yet to explain these deviations.

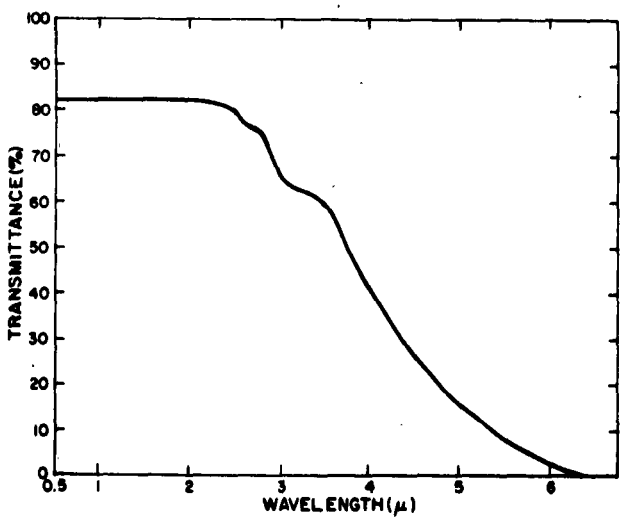

Fig. 6. Infrared absorption caused by free carriers in n-type ZnSe crystals.

3. Hot-Cold Argon Gun to Prepare Surface Junctions

To enable us to prepare p-type layers on n-type ZnSe and CdS crystals or n-type layers on p-type ZnTe by surface diffusion, a device suggested by Grimmeiss (personal communication) was constructed, and is shown in Fig. 7. A hot argon stream heats the surface of the crystal, whereas the bulk remains cool due to the effect of a heat sink. After the dope has diffused far enough, the surface is abruptly cooled to lock the acceptors into the crystal lattice in their high-temperature state, prohibiting precipitation or coagulation. Results will be related in the next report.

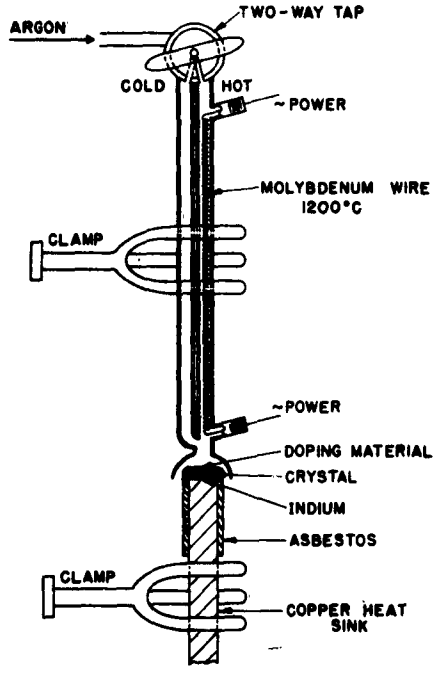

Fig. 7. Hot-cold argon gun for surface junction preparation in II-VI compounds.

F. N-TYPE ZnTe*

By all normal growth methods, ZnTe crystals of p-type conductivity are obtained, even if foreign acceptor impurities like Cu or Ag are absent. This is due to a innate tendency of ZnTe to form Zn vacancies which act as double acceptors.

Zinc pressures of a few atmospheres as available in our melt-growth methods are not sufficient to prevent the formation of zinc vacancies. To provide higher zinc pressures, the small

*Work done by A. G. Fischer

autoclave described in Fig. 2, p. 6, Scientific Report No. 1, AFCRL 360, was put into operation again. An Alundum tube was filled with 100 grams of spectroscopically pure zinc, 10 grams of spectroscopically pure tellurium and 1 gram of spectroscopically pure aluminum, and inserted into the autoclave. The autoclave was carefully flushed with argon and pressurized with argon to 200 atmospheres. Then the temperature of the Alundum was brought to 1350°C. The vertical Alundum tube, which was closed at the lower (hot) end and cool at the upper, open end, acted as a reflux system, preventing the excape of zinc. In this way, ZnTe formed in a zinc flux under 200 atm. of zinc pressure. After cooling, the excess zinc was removed with HCl. The bright-red ZnTe crystals (average sizes of 1 mm) showed n-type conductivity under thermoelectric microprobes. As soon as larger crystals are available, Hall effect measurement will be undertaken to confirm this result.

II. TUNNEL INJECTION ELECTROLUMINESCENCE (TIEL) AND RELATED TOPICS

A. BRIEF RECAPITULATION OF THE PRINCIPLE

In the last report (AFCRL 62-588, p. 94) we described the new principle of tunnel-injection electroluminescence. Instead of graded-gap, quasi-homogeneous p-n junctions, which had been recognized as the ideal solution[5] but which are very difficult to prepare, especially in II-VI compounds which are nonamphoteric, we use a heterogeneous junction between a luminescent semiconductor and a wide-gap semiconductor of the opposite type and higher bandgap than the luminescent material, with an interposed insulator layer. As illustrated in Figs. 13 and 14 of the previous report, we get an efficient tunnel injection contact which prohibits tunnel extraction. Fabrication is easy because no single crystals are required. In the following, our efforts to reduce this idea to practice will be described.

B. PRELIMINARY EXPERIMENTAL RESULTS ON TIEL*

The first experiments were performed with selected Eagle Picher CdS single crystals which were n-type and luminescent. When these crystals were contacted with Ga-In alloy on one side and silver paste on the other, they showed red electroluminescence when the silver paste was positive. Evaporated silver did not perform. However, if the crystals were coated with a potassium silicate layer, or a silico-organic film, of very low thickness (below the thickness of the first interference fringe), then the effect was obtained. At liquid nitrogen temperature, an ice film was found to be suitable as insulating barrier. In the case of silver paste, the lacquer acts as a thin insulating tunnel-barrier.

Instead of using single crystals, extended polycrystalline films seemed to hold more promise for applications. Thin, conducting and luminescent CdS films were produced on tin-oxide-coated substrates by vacuum evaporation and afterbaking, either in a packing of activated CdS powder, or simply in an inert atmosphere.

The CdS film was then covered with a thin insulating film by evaporating CaF_2 in vacuum. Several other methods of preparing the insulating film are presently under study, including oxidation of metal films, electrolytically formed films and chemically formed films.

The insulating film is then covered with a wide-bandgap, p-type semiconductor. Cuprous iodide was, so far, the most convenient material. Films can be prepared either by evaporation of CuI, or by evaporation of Cu and subsequent exposure to iodine vapor.

*Work done by H. I. Moss, R. Peterson, and A. G. Fischer

The structures are rectifying and show electroluminescence under forward bias, though not very bright and efficient as yet.

C. LIGHT EMISSION FROM HETEROGENEOUS p-n JUNCTIONS IN CdS*

At liquid nitrogen temperature, the CuI-CdS structures show emission of red light under forward bias and also if the insulating CaF_2 film is missing. Whether this is caused by injection in an abrupt p-n junction, or by tunnel injection through an unidentified insulating interlayer, is not established as yet.

Another experiment involved the formation of a junction between luminescent CdS films and the arsonium salt of TCNQ, a very conductive, p-type semiconductor. This organic semiconductor has the peculiarity that it has no conduction band. It extracts electrons from the valence band of the material it is brought in contact with. The TCNQ was melted onto the CdS film and a low resistance contact was made to the TCNQ by means of silver paste of Ga-In alloy. Application of 10 volts dc and 2-4 ma, TCNQ positive, results in red light emission beneath the TCNQ contact at room temperature. The TCNQ is serving as a hole-injecting contact.

D. ELECTRICAL MODULATION OF PHOTOLUMINESCENCE IN CdS FILMS**

When it was attempted to inject holes from an electrolyte, it was discovered that the photoluminescence output of a UV-excited CdS-film deposited on conducting glass can be modulated by the voltage applied between the conducting glass which served as a back electrode, and the aqueous electrolyte which served as a front electrode. The UV was 3650 Å from a mercury lamp. If the electrolyte was negative with respect to the CdS, permanent quenching of photoluminescence to about 1/10 the initial brightness was observed. If the electrolyte was positive, enhancement by a factor 2-3 over the field-free condition was noted.

A tentative explanation of the phenomenon is that the electron-hole pairs which are generated by light absorption are either separated or brought together by the field in the barrier, depending on polarity of the applied voltage. In one case, radiative recombination is enhanced, in the other reduced.

*Work performed by H. I. Moss and R. Peterson
**Work done by H. I. Moss

III. EXPLORATION OF WIDE-GAP III-V COMPOUNDS*

A. MISCIBILITY OF GaP, AlP, BP, GaN, AlN AND BN

In the last report our results on the apparent nonmiscibility of GaP and BP were related. This result is of importance because we had hoped to be able to enlarge the bandgap of GaP by BP additions to obtain green and blue emission with better temperature stability. This is not possible.

1. AlP – BP

The next logical step is to test AlP (bandgap about 2.5 ev) for miscibility with BP (bandgap 5.9 ev). If such mixtures were existent, it might be possible to improve the poor chemical stability of AlP, since BP is chemically very stable. At first, the lattice constant of AlP had to be established.

AlP was prepared by rf-heating aluminum of 99.9999% purity in a boron nitride crucible with tungsten susceptor (see last report, p. 85) at 20 atm. phosphorus pressure to 1650°C for ½ hour. Light-yellow crusts were obtained which were strongly photoluminescent (orange) at nitrogen temperature.

X-ray analysis (R. J. Paff) showed that the samples were a cubic material with a lattice constant of 5.4636 Å, which is larger than the value of 5.451 Å in the ASTM file which is based on a paper of Addamiano. This result was obtained repeatedly. Also, the crystals which were prepared earlier in cooperation with R. Guire by reaction of $AlBr_3$ with PH_3 had shown the larger lattice constant. Recently, D. Richman submitted halogen-transport-grown AlP crystals for X-ray analysis, and again the large value was found.

After the lattice constant of AlP had been established, melts of aluminum with additions of crystalline boron (99.9999%) were heated in phosphorus vapor, as before. X-ray analysis yielded the unchanged lattice constant of AlP, with lines of boron, aluminum and boron phosphide superimposed.

The lattice constant of boron phosphide, taken from the ASTM file, coincides exactly with the values obtained by X-ray analysis of a boron phosphide crystal obtained from Monsanto Chemical Co. through the generosity of Dr. Ruehrwein. The lattice constant is 4.5380 Å.

It must be concluded that AlP and BP are not miscible, at least not under the conditions that prevailed in our experiment.

*Work performed mainly by A. G. Fischer

2. GaP – AlP

The lattice constants of these two compounds are exactly equal, so that X-ray determination of miscibility is not easily possible. We are presently studying the crystal habits of crystallites under the microscope to determine mutual miscibility.

3. BN – AlN

A mixture of aluminum powder and 30 wt-% boron powder was heated to 1800° in forming gas (90% N_2, 10% H_2) for two hours. The resultant powder showed only the lines of AlN, although chemical analysis (S. Adler) revealed that the 30% boron was still present. Possible explanations which are presently under study include: (a) The boron nitride is in a very fine-dispersed state so that it does not show up on the X-ray film; (b) BN, which normally has a graphitic structure, but also exists in a cubic, high-pressure modification (with a smaller lattice constant than the c-value of hex. AlN), forms a solid solution with hexagonal AlN without changing the lattice constant of AlN.

4. GaN

Miscibility of GaN with other compounds is difficult to determine because GaN decomposes above 1000°C, even if 2000 atm. nitrogen pressure is applied to prevent decomposition.

B. ELECTROLUMINESCENCE AND OTHER PROPERTIES OF BP

Small BP crystals given to us by Dr. Ruehrwein of Monsanto are brown, indicating the presence of impurities. The pure material should be colorless. Spectrographical analysis (H. Whittaker) revealed a high concentration of nickel. From this it can be concluded that the crystals were grown from a nickel flux. The crystals are p-type and very conducting. By contacting with various metal probes it was found that the crystals show red electroluminescence, always at the negative contact. This injection electroluminescence persists even if the crystal is current-heated to incandescence temperature. The efficiency is extremely low, worse than that of the impact-ionization EL-ZnSe crystals.

At present, several approaches toward obtaining better BP crystals are being investigated.

IV. BASIC STUDIES OF ZnSe FILMS MADE BY VACUUM TRANSPORT*

The investigation of the properties of vacuum transported ZnSe films, which was started in the last report, was continued. In the last report period, a new evaporator which permits better control was completed and has been extensively used.

A. EVAPORATION OF FILMS

The essentials of the high-temperature, multiarm evaporation chamber used during the past six months are shown in Fig. 8. There are five side arms at the bottom of the chamber. Three are short and inclined 13° to the vertical to point toward the substrate. These are used to evaporate

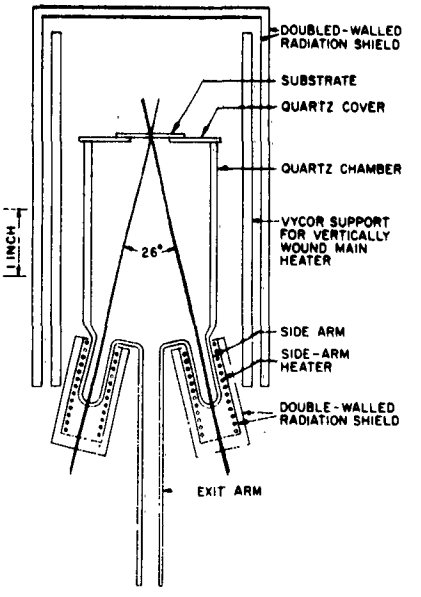

Fig. 8. Multiarm evaporation chamber.

high-temperature charges. Two are long and vertical. One of these is closed and is used to evaporate low-temperature charges. The other, the exit arm of Fig. 8, is open. It serves to evacuate the chamber to the bell jar enclosing the whole assembly. Each of the four evaporating side arms has its own tungsten-coil heater and radiation shield. The main chamber also has a heating coil and radiation shield. This main coil is wound vertically, much like that of a toaster, on a 5¼ in. long Vycor cylinder. The large main heater uses powers, voltages, and currents of the order of 200 watts,

*Work performed and section written by W. H. Fonger

100 volts, and 2 amperes, respectively. The small side-arm heaters use corresponding quantities of the order of 40 watts, 4 volts, and 10 amperes, respectively. The chamber is removed for cleaning and loading by retracting the inclined side-arm heaters downward, removing the radiation shield of the main oven upward, and then removing the chamber upward. The substrate was usually Pyrex although any convenient flat plate or wafer can be used. Photographs of the system in increasing disassembly states are shown in Figs. 9 through 12.

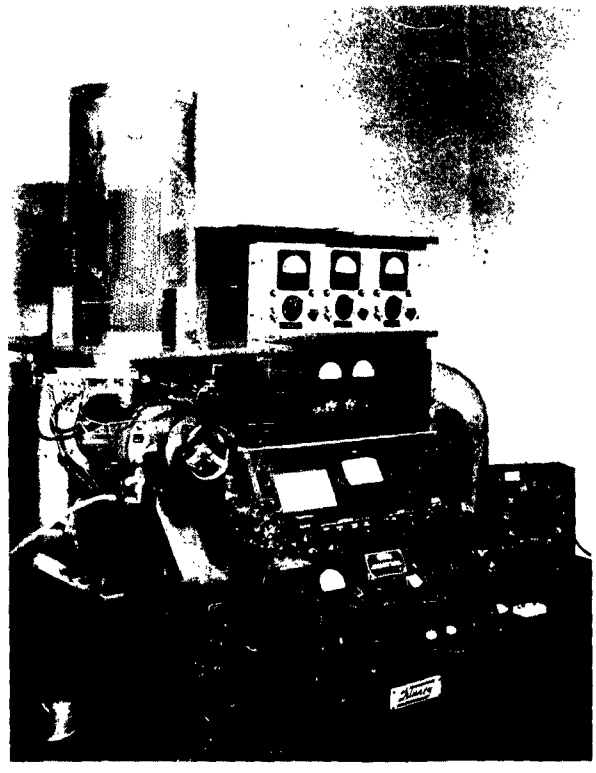

Fig. 9. Evaporation equipment.

The temperature throughout the main chamber is uniform within a few degrees except for the curved bottom of the chamber which is slightly cooler. Materials evaporated into the chamber which have a very low sticking probability at the chamber temperature tend to deposit preferentially on its curved bottom surface or, if sufficiently volatile, pass out of the chamber and deposit on the walls of the exit arm. For example, any appreciable nonstoichiometric excess of ZnSe deposits as free Zn or Se in the exit arm for oven temperatures greater than 400°C.

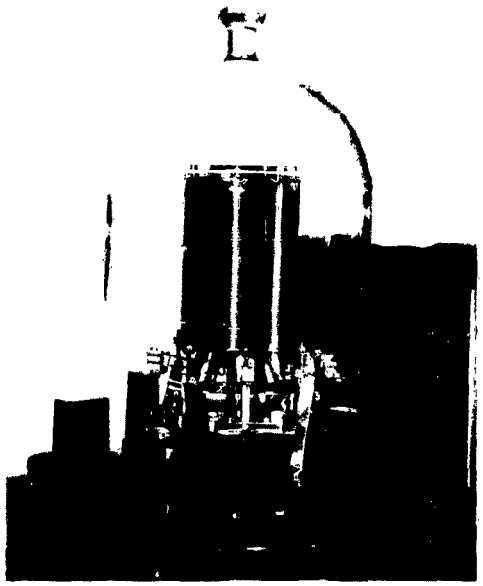

Fig. 10. Close-up view of evaporating bell jar.

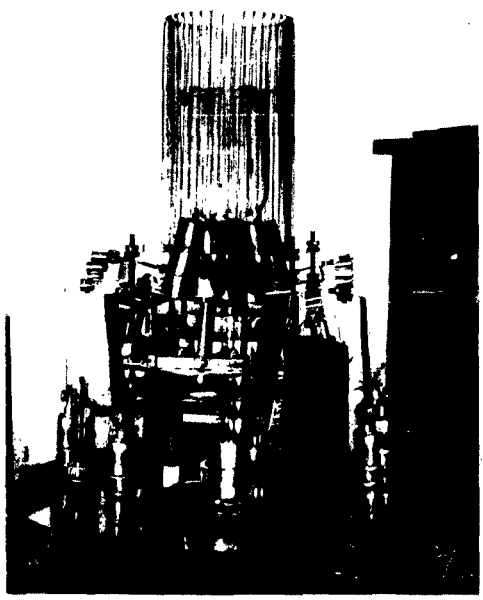

Fig. 11. Close-up view with bell jar and radiation shield of main oven removed.

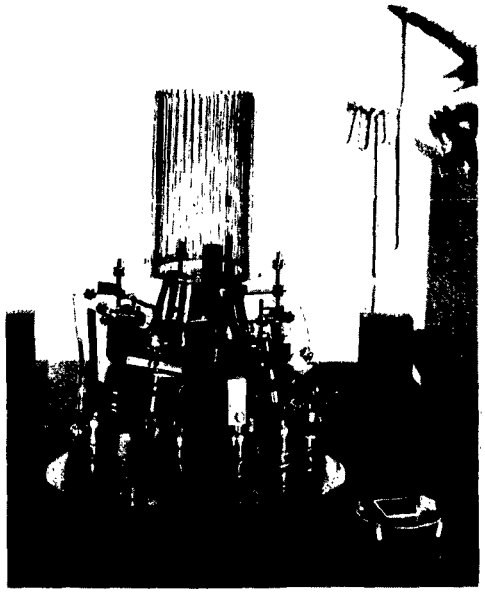

Fig. 12. Close-up view with slanted side-arm heaters retracted and chamber, chamber cover, and substrate removed.

Power fed to the side-arm heaters couples into the main oven and affects its temperature. However, the power to the main heater can be reduced slightly to compensate this, and the temperature of the main oven can be maintained within a 5°C range while side-arm heaters are turned on and off. The temperatures of the side arms are coupled to that of the main oven but not to each other. Thus, since only a few main-oven temperatures are used, the temperature vs. input-power curves of the side-arm heaters can be calibrated at each main-oven temperature.

The heat capacity of the main oven, dominated by the 200-gm. mass of the Vycor cylinder, is large. This is helpful in maintaining the constancy of the main-oven temperature when turning side-arm heaters on and off. It is inconvenient at shut-down because the temperature decays slowly. Probably the optimum heat capacity is lower.

As might be expected for a closed system of this type, the yield at the substrate is rather insensitive to oven (substrate) temperature. For ZnSe, it goes through a broad minimum near 580°C of 11 micron layer thickness per evaporated gram. The yield reaches 15 μ/gm at 330°C on the low side and at 700°C on the high side. The rise on the low side is due to the evaporating beam

being directed toward the substrate. The rise on the high side is probably due to the substrate being just slightly cooler than the vertical walls of the chamber. ZnSe films can still be deposited at 800°C, but on quartz such films are full of pinholes.

B. LIGHT SCATTERING

ZnSe films evaporated on glass had the structure shown in Fig. 13. The bottom side of the film lies flat on the glass. The top surface reflects the advance of crystallite growth from the substrate and is faceted. If the temperature of the substrate is increased, the size of the crystallites increases, and the facets forming the top surface enlarge. Light scattering takes place at the faceted surface and increases steeply with facet size. At low substrate temperatures, the linear dimensions of the facets are small compared with optical wavelengths, and the scattering is Rayleigh scattering. At high temperatures, their linear dimensions are large compared with optical wavelengths, and the light scattering becomes just ordinary reflection and refraction at a multitude of inclined crystallite faces.

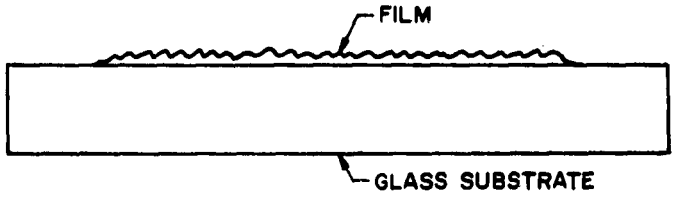

Fig. 13. Film structure.

Simple qualitative observations on films formed at the highest temperatures support this picture. If such a film is placed film-side down on a black background in window light, the specular reflection is greater than that from glass alone and is white, but the diffuse reflection is a fairly saturated yellow. Specular reflection occurs at the upper, flat film-glass interface and occurs approximately equally at all wavelengths. Diffuse reflection occurs at the lower faceted surface and reaches the observer only after the light has made a double pass through the film. This pass absorbs all blue light above the ZnSe bandgap (2.7 ev) and renders the passed light yellow. If the film is turned film-side up, there is no specular reflection, and the diffuse reflection is very pale yellow, practically an off-white. The specular reflection is destroyed at the faceted top surface. A good fraction of the diffuse reflection occurs at the first encounter with this faceted surface. It occurs approximately equally at all wavelengths and reaches the observer without any yellowing pass through the film, thus resulting in the whitish diffuse reflection.

The same experiment can be done somewhat more dramatically, if a beam of blue light (through a Wratten 47 filter) is passed through the film in a dark room. Light through this filter spans the ZnSe bandgap. If the film is placed glass-side to the beam, the specular reflection (greater than from glass alone) is the same color as the incident light. The diffuse reflected and transmitted lights, which scatter from the far, faceted film surface, are both very green (not really, but relatively) compared to the incident light. If the film is turned film-side to the beam, the specular reflection disappears, the diffuse transmitted light is again green, but the diffuse reflected light is only slightly greener than the incident light. The explanations are the same as above. Light trapped in the glass by total internal reflection and leaked at its edges always makes a pass through the film and is green for either orientation of the film.

If a film formed at the highest temperatures is held in a beam of strong sunlight and gently rocked, the diffuse reflection is seen to be uneven and to sparkle from many points distributed randomly over the film. These sparkles are specular reflections from tiny facets which chance to be rocked through the proper orientation for mirror reflection. Under the microscope, one sees the entire film to be composed of tiny crystallites with linear dimensions of the order of a few microns. This agrees with the observation that the Rayleigh scattering at very long wavelengths becomes appreciable at a few microns.

To study the light-scattering effect quantitatively, the scattering box shown in Fig. 14 was constructed. Light from a microscope illuminator two feet distant is passed through the aperture

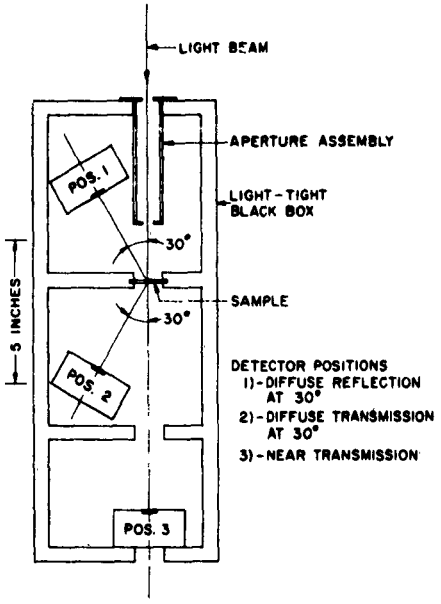

Fig. 14. Box for measuring light scattering.

assembly, through the film, and out the far end of the box. The film is inserted through a port in the top of the box. The detector is the S1 photocell head of a Welsh Densichron with a Wratten 26 filter covering the photocell. The filter cuts off the response below 0.60μ. The photocell responds from this wavelength to 1.1μ, peaking strongly at 0.8μ. The detector may be positioned to record 1) the diffuse reflection at 30°, 3½ in. from the film, 2) the diffuse transmission at 30°, 3½ in. from the film, and 3) the "near" transmission, 8 in. from the film. During measurement, ports over the film and detector positions are covered. Measurements of "far" transmission and "far" specular reflection at 0° were also made. These did not require reproducible positioning of the detector and were made outside the box in a darkened room. For diffuse reflection and transmission, the sensitivity of the detector was adjusted to read 79 per cent for the diffuse reflectance from a white card. For specular reflection, the sensitivity was adjusted to read 8 per cent for the specular reflectance from a Pyrex slide.

The results for many "proper" ZnSe films are shown in Fig. 15 as a function of the substrate temperature during film formation. From thermodynamic considerations, the transmission at 0° must be the same for the film oriented either toward or away from the beam, and this was indeed observed

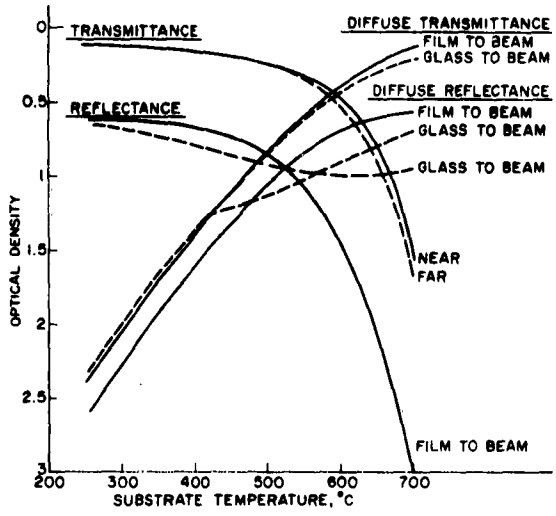

Fig. 15. Light transmission and reflection.

in all cases. The general argument does not apply to reflection or to transmission at 30° arising from 0° incidence, so that specular reflection and diffuse reflection and transmission can be and, in general, were different for the two orientations of the film.

With films formed at low temperatures, the scattered light is small, and the specular reflection and transmission are those of a flat film of index 2.5 on flat glass of index 1.5. The reflectance and transmittance of such a system, neglecting interference effects,* are 0.602 and 0.125, respectively, in optical density units, in good agreement with the observations at low temperatures.

With films formed at higher temperatures, the scattering becomes larger, and the specular reflection and transmission become those of a faceted film of the kind shown in Fig. 13 of index 2.5 on flat glass of index 1.5. As the faceted surface of the film becomes extremely scattering, the specular reflectance and transmittance of such a system tend toward zero except that the specular reflectance for the glass-to-beam orientation tends toward 1.012, in optical density units, all in reasonable agreement with the observations at higher temperatures.

The diffuse reflectance and transmittance can be calculated in the case of very large scattering (high substrate temperature) where the scattering is ordinary reflection and refraction at a collection of diversely oriented crystallite faces. The $(n_1 - n_2)^2/(n_1 + n_2)^2$ formula for normal reflectance is approximately valid to rather large incidence angles. We use this formula at all angles. To this approximation, for the orientation film-to-beam, the reflectance and transmittance of a faceted film of the kind shown in Fig. 13 are identical with those of a flat, nonscattering film of the same index except that these quantities are diffuse in the first case, specular in the second. In agreement with this consideration, the diffuse reflectance and transmittance of films grown at 700°C in Fig. 15 are seen to agree well with the corresponding specular quantities at low substrate temperatures. Indeed, the compressed scale of Fig. 15 does not do justice to the agreement. The observed diffuse reflectance and transmittance for 700°C films for the film-to-beam orientation were 0.57 ± .01 and 0.13 ± .02, respectively, in optical density units. These are to be compared with the values 0.602 and 0.125, respectively, quoted above for the corresponding specular quantities for flat films. For the orientation glass-to-beam, the diffuse quantities of films formed at 700°C are somewhat smaller because some of the incident light is lost to specular reflection.

Incidentally, from the model here for scattering from very high-temperature films, for the film-to-beam orientation, 26 per cent of the diffuse reflected light makes passes through the film, 74 per cent never enters the film. This is the detailed explanation for the qualitative observation above that light through a Wratten 47 filter is rendered only faintly greener in diffuse reflection from such a film.

Rayleigh scattering from small objects is symmetric front and rear. Thus one might expect the diffuse reflectance and transmittance to approach each other in films formed at low substrate

*The reflectance and transmittance of a flat film oscillate with wavelength due to interference effects. However, the average effect is approximately that which would be calculated neglecting interference. The detector here averages over a wide band from 0.6 to 1.1μ.

temperatures. This approach is realized fairly well for the glass-to-beam orientation but falls short by approximately 0.20 optical density units (a factor of 1.58) for the film-to-beam case. Also see Fig. 16 below. Presumably a proper treatment of Rayleigh scattering at a faceted interface could account for this.

At low temperatures where the diffuse reflectance for the film-to-beam orientation is smaller than the other diffuse quantities, the specular reflectance is higher for this orientation. This is indeed necessary because, since 0° transmission must be the same for either orientation, a lower scattering for one orientation can only be balanced by increased specular reflection at the same orientation. At higher temperatures where the specular reflection reverses and becomes larger for the glass-to-beam orientation, the scattering also reverses and becomes smaller for this orientation.

For films formed at intermediate substrate temperatures, the scattering passes through the region (difficult theoretically) where the wavelength is comparable to crystallite size. The experimental curves, however, proceed rather smoothly through this region. The diffuse reflectivity in the glass-to-beam orientation is an exception; it behaves differently. Ratios of diffuse quantities are shown in Figs. 16 and 17 on an expanded optical density scale. The plotted points show standard deviations over many films. The different behavior of the diffuse reflectivity in the glass-to-beam orientation at intermediate temperatures shows up as a strong change in any ratio involving this quantity. This different behavior is not interpreted by us.

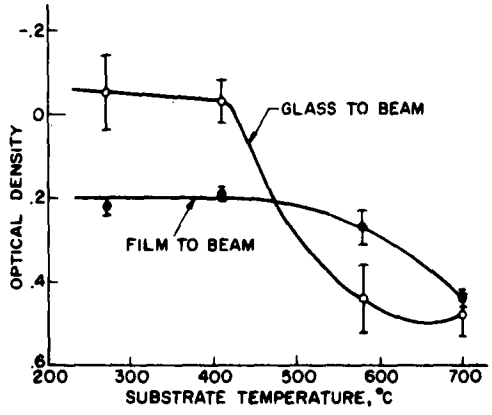

Fig. 16. Diffuse reflectance/ Diffuse transmittance.

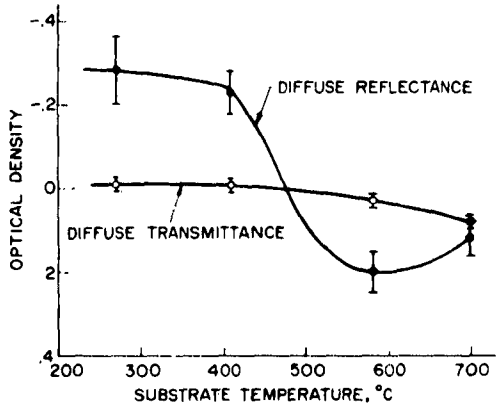

Fig. 17. Glass to beam/Film to beam.

We use the curves in Fig. 15 to assign effective substrate temperatures T_E to films. That is, films are assigned a T_E according to how they scatter light. Proper films are those for which T_E is the same as T_A, the actual substrate temperature. A doped film in which the dope affects crystallite growth will scatter light differently from proper films prepared at the same temperature, and its T_E will differ from its T_A.

The T_E assigned to a film is independent of which curve in Fig. 15 is used for the assignment provided a) the curve varies rapidly enough with temperature to permit accurate assignment and b) small but probably significant differences in T_E of 25 degrees or less are ignored. That is, the reflectance and transmittance quantities of *any* film lie fairly close to the intersections of the curves in Fig. 15 with some particular temperature abscissa T_E. Usually we use the diffuse-reflectance and diffuse-transmittance curves for the film-to-beam orientation. These curves rise smoothly and steeply with temperature, although they do saturate at high temperatures where the scattering becomes normal reflection and refraction. The peculiar diffuse reflectance for the glass-to-beam orientation varies weakly with temperature over a wide range. Moreover, this quantity does not correlate so well with the others. Note in Figs. 16 and 17 that the standard deviations of ratios involving this quantity are larger than those of other ratios. The diffuse transmittance for the glass-to-beam orientation correlates so well with that for the film-to-beam orientation (Note the small standard deviations for the diffuse-transmittance ratio in Fig. 17) that it is redundant to use both. The 0° transmittance varies weakly with temperature below 450°C and is not usable in this range with the measurements here.* Some use of 0° transmittance will be made at higher temperatures.

As was carefully established previously[6] from 0° transmission measurements, the Rayleigh scattering of films made at 410°C (and therefore surely at any low temperature where the scattering is small) is proportional to the thickness of the film. This must be due to the fact that, for a given substrate temperature, the size of the crystallites and of their facets increases with film thickness. This is likely true at all temperatures. S. G. Ellis[7] of these laboratories, working with high-temperature films of GaAs, has observed from microscope studies that the lateral extent of crystallite faces increases with film thickness.

This thickness effect on scattering complicates the assignment of T_E. At low temperatures where the scattering is proportional to t, the optical densities of diffuse quantities are corrected to a standard thickness t_o (1μ here) by the addition $\log_{10}(t/t_o)$. This correction was used at 410°C. At this temperature, for proper films in the film-to-beam orientation, $\log_{10}(t/t_o)$ correlated −0.874

*This range is usable if better measurements are made. In the last report, it was shown that the scattering of 410°C films accounts accurately for transmission losses in excess of those due to specular reflection. Thus scattering and transmission could be used equivalently. However, transmission measurements in that case were accurate to better than 0.01 optical density unit because a split-beam method was used and interference effects were carefully eliminated.

and −0.848 with the raw optical densities of diffuse reflectance and diffuse transmittance, respectively. A somewhat smaller correction was used at 580°C, and no correction was used at 700°C. When the scattering saturates at high temperatures, the thickness effect must disappear. Some attempt had been made to make the thicknesses of high-temperature films approximately standard. Thus the thickness corrections at 580°C were small, and their validity could not be established from the data.

Different assignments of T_E from different Fig. 15 curves are illustrated in Fig. 18 for the films prepared at 580°C. The abscissa is the T_E assignment derived from diffuse transmittance

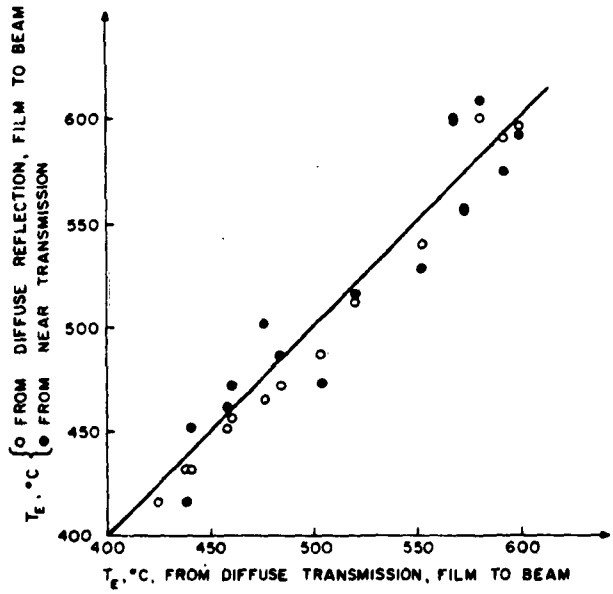

Fig. 18. Effective substrate temperatures of films prepared at 580°C.

in the film-to-beam orientation. The ordinate is the same T_E assignment derived from either diffuse reflectance in the same orientation (open circles) or near transmittance (dark circles). The different assignments are seen to be equal if differences of 25 degrees or less in T_E are ignored.

Mean T_E assignments for many films prepared at 410°C, 580°C, and 700°C are shown in Fig. 19. Many films are proper, that is, lie along the line T_E (ordinate) = T_A (abscissa). At each preparation temperature, these proper films are grouped together and represented by the standard deviation bar for the group. A similar grouping has been made for five (Ag + In)-doped films. The

other films are shown singly. The improper films here all fall in the half-plane $T_E < T_A$. That is, the dopes* used in these films inhibited crystallite growth. In the cases of Zn-doped films at 580°C and $ZnCl_2$- and In-doped films at 700°C where different values of T_E are obtained for different films, the smaller T_E values (more inhibited crystallite growth) are always associated with greater doping.

The fact that a given dope can affect crystallite growth differently at different temperatures need not be surprising. The case of NaCl is a good example. As will be shown below, coevaporation of ZnSe and NaCl in the mass proportion 10:4 at 700°C produces a self-activated ZnSe luminescence. Only a small amount of Cl is incorporated into the film, and the bulk of the NaCl flushes out of the hot chamber. If the same procedure is used at 580°C, the NaCl remains in the chamber, settles on the substrate, and destroys the film.

From the data shown in Fig. 19, it appears that Cl per se does not inhibit crystallite growth. Excess Zn does, either in the form of Zn or $ZnCl_2$, but its effect is lessened at higher temperatures where Zn or $ZnCl_2$ flush rapidly out of the chamber. Ag, perhaps especially in approximately equal proportion with In, inhibits crystallite growth at 580°C. Cu, either in the form of Cu or $CuCl_2$, shows little effect at 700°C. Indium is peculiar. The same concentration that inhibits crystallite growth at 700°C does not at 580°C. In fact, the following subtle difference was observed: For the two In-doped films prepared at 580°C, the T_E's assigned from diffuse reflectance were approximately 25 degrees higher than those assigned from diffuse transmittance. For the two In-doped films prepared at 700°C, the reverse was true. A large Se excess at 580°C does not affect crystallite development; this is understandable, since Se is so volatile at this temperature.

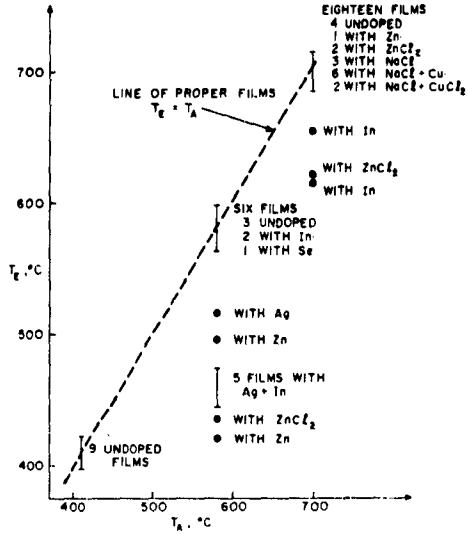

Fig. 19. Effective vs. actual substrate temperatures.

*Dope as used here really means coevaporant. Chemical analyses of the films were not made, and the degree of dope incorporation into the host is uncertain.

The forward scattering measured here 30° from the beam spreads over all angles, including 0°. Thus a 0° transmission measurement inherently sums scattered and unscattered lights. For 700°C films, the near transmission position in the scattering box of Fig. 14 is evidently not far enough to escape scattered light since for this case near transmittances proved to be larger than far transmittances by ≈0.11 optical density units.

C. LUMINESCENCE

The ZnSe films prepared thus far have been rather resistive, so that it has been convenient to use photoluminescence to guide the preparation. The best, reproducible luminescence obtained to date is the red-orange "self-activated" luminescence coactivated by Cl. The spectral-distribution curve has been given by Leverenz.[8] It peaks at 0.65μ. The film is prepared as follows: ZnSe and NaCl, in the mass proportion 10:4, are coevaporated from separate side arms of the chamber (Fig. 8) with the chamber (and substrate) at 700°C. The ZnSe coats the substrate and the entire chamber. A proper amount of Cl is incorporated into the film, but the bulk of the NaCl flushes out of the hot chamber and deposits along the walls of the cool exit arm. The films on the substrate and on the chamber walls and cover are equally luminescent and luminesce equally for excitation from either side (film or glass). The substrate is Pyrex, but the chamber and its doughnut-shaped cover are quartz. Thus large differences in substrate contraction during cooldown do not affect the luminescence.

The excitation spectrum for photoluminescence (measurement kindly provided by R. E. Shrader) peaks sharply just on the long-wavelength sides of the band edge (2.74 ev), just as does the excitation spectrum for ZnSe photoconductivity.[9] The reason is the same for either case: Below the band edge, the excitation simply is not absorbed; above the band edge, the excitation is absorbed very close to the surface where surface effects decrease the luminescence efficiency and the photoconductivity sensitivity. Thus it has been convenient to excite photoluminescence with a band of blue light spanning the band edge. This is obtained with a microscope illuminator and filter consisting of $CuSO_4$ solution and a Wratten 47 filter. The lamp output is varied with a variac, and the intensity of the blue light is calibrated (in relative units) with an S4 photocell.

Figure 20 shows, for an efficient film, the variation of red luminescence with the intensity of blue excitation. The curve is superlinear at low excitation levels and practically linear at high excitation levels. The luminescence was measured with an S1 photocell covered with a Wratten 26 filter to exclude the exciting light.

Figure 21 shows the efficiencies of the best films to date relative (in log 10 units) to that of top-quality ZnSe: Cu(.01), [NH_4 Cl(2)] powder phosphors. These powders were prepared by W. M. Anderson in 1954 during an optimization program. They are sufficiently efficient as to appear

red when illuminated with blue light. The spectral distribution of the Cu-activated luminescence is practically the same as that of the self-activated material,[10] so that a given detector measures both luminescences equally. The efficiencies in Fig. 21 were measured at constant luminescent output. Two blue light beams were incidenced on two adjacent films: the test film and a standard. The light to the standard was maintained fixed, and that to the test film was adjusted until both films appeared equally luminescent as seen through a Wratten 26 filter to exclude exciting light. The efficiency of the test film is inversely proportional to the excitation intensity required for the match. The eye matching can be done very accurately. The level of luminescent output used was that indicated by the arrow in Fig. 20. The efficiencies of several of the films were remeasured at constant excitation intensity with 0.365μ ultra-violet. The luminescent output in this case was measured with an S1 photocell covered with a Wratten 26 filter. The results reproduced those shown in Fig. 21 very closely.

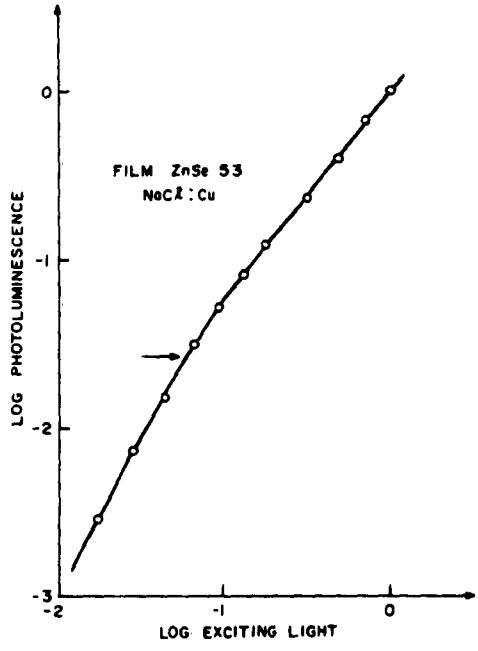

Fig. 20. Photoluminescence vs. excitation intensity.

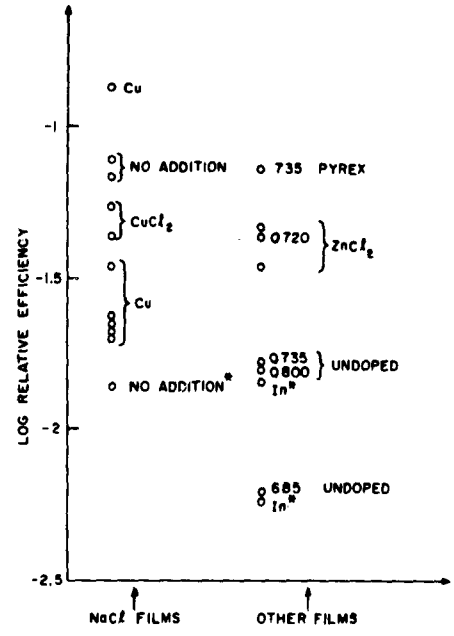

Fig. 21. Photoluminescence of films relative to good powder.

The films in Fig. 21 are separated into two groups: the left group consists of films made by the NaCl method; the right group are films made by other methods. Consider the NaCl group: The substrate temperature was always 700°C. Dopes used in addition to NaCl are indicated for

individual films. ZnSe and NaCl were always evaporated in the mass proportion 10:4, except for one film indicated by an asterisk. In this case, ZnSe and NaCl were evaporated in the mass proportion 100:1, and the efficiency proved to be the lowest of the group. If no NaCl is used, the efficiency lies near the −2.5 level at the bottom of the figure. The reproducible level of self-activated luminescence is exhibited by the two films labeled "no addition" near the level −1.15. Addition of $CuCl_2$ decreased the efficiency somewhat, and addition of Cu decreased it even more, except for one case which yielded the best luminescence to date. This exception could not be repeated and will be ignored here.

According to Leverenz's powder data,[10] in going from self-activated to Cu-activated ZnSe luminescence, one could expect to increase the efficiency of photoluminescence by the factor 45/8 (0.75 log units). Since this increase has not been accomplished here, it is concluded that Cu has not been incorporated into the films properly. Accomplishment of this increase would yield films only 0.40 log units below the best powders. Moreover, the test conditions here favored the powder samples slightly so that the difference would be even less.

For films of the non-NaCl group, substrate temperatures other than 700°C were sometimes used, and these temperatures are indicated in Fig. 21 for individual films. Prefix *Q* means quartz substrate. The dopes used are also indicated. The most efficient film of the group is listed as doped by Pyrex, and this is literally true. The Pyrex substrate was inadvertently taken to 735°C, and the film fused into the Pyrex. The film-Pyrex interface was gradual and gave no specular reflection. This fusing seems to have been essential for the good luminescence. The quartz chamber and cover supporting the substrate were much less luminescent. The result could not be duplicated on Pyrex at somewhat lower temperatures nor on quartz at the same or higher temperatures. This method of inducing luminescence seems uninteresting. The next most efficient films were a group of three doped with $ZnCl_2$. This is probably the same self-activated Cl-coactivated luminescence induced with NaCl, but less efficient because of the inhibiting action of excess Zn on crystallite growth. The next most efficient films were two undoped films temperature-activated on quartz above 700°C and one In-doped film prepared at 700°C. Another film more heavily doped with In gave a lower efficiency. This film fell near the −2.5 level characteristic of undoped films temperature-activated at 700°C.

Except for the two In-doped films indicated with asterisks, the films of the non-NaCl group had a common undesirable feature – the luminescence excited from the glass side was appreciably less than that excited from the film side. It is the larger, film-side luminescence whose efficiency has been portrayed in Fig. 21. Contrary to this, for the NaCl group, the luminescence was always the same for excitation from either side, except in one case indicated by an asterisk where the

efficiency from the glass side was lower and where, as noted previously, only 1/40 of the standard amount of NaCl was used. These remarks apply also to films on the chamber walls and cover. For the NaCl method, such films were equally luminescent for excitation from either side. For non-NaCl methods, they were less efficient for excitation from the glass side. Thus, all considerations taken together, none of the non-NaCl methods appear at all promising for good luminescence compared to the NaCl method.

Films prepared at temperatures 580°C or lower were all very inefficient – below the –2.5 level of Fig. 21. In these cases, local regions of good luminescence were sometimes obtained in the bottom of the evaporation chamber in regions of strong temperature gradients. One common location was the neck of the exit arm where it joins the main chamber. Thus good luminescence can be achieved at temperatures below the 700°C range shown in Fig. 21. However, the conditions needed for the luminescence appear to be less straightforward than those required at 700°C.

ACKNOWLEDGMENT

W. H. Fonger thanks Dr. R. E. Shrader for many helpful discussions during the course of the work.

REFERENCES

1. S. Larach, R. E. Shrader, and C. F. Stocker, Phys. Rev. **108**, 587 (1957).
2. W. W. Piper and F. Polich, J. Appl. Phys. **32**, 1278 (1961).
3. N. Holonyak, D. C. Jillson, and S. F. Bevacque, *Metallurgy of Semiconductor Materials* **15**, 49-59, Interscience 1962.
4. East European Luminescence Conference, Nidice Castle, Sept. 1962, as related by R. Nitsche.
5. A. G. Fischer, J. Solid State Electronics **2**, 232 (1962).
6. A. G. Fischer, W. Fonger, and A. S. Mason, Semiannual Scientific Report No. 2. Contract No. AF 19(604)8018, August 15, 1962, p. 113.
7. R. R. Addis, S. G. Ellis, W. L. Hui, H. J. Moss, G. Noel, and P. Vohl, Contract No. NAS 7-202, Dec. 31, 1962, p. 4.
8. H. W. Leverenz, *An Introduction to Luminescence of Solids*, (John Wiley and Sons, Inc., New York, 1950), p. 200, Curve 9.
9. R. H. Bube and E. L. Lind, Phys. Rev. **110**, 1040 (1958).
10. H. W. Leverenz, op. cit., Compare Curve 9, p. 200, with Curve 4, p. 202.

Electronic Research Directorate, A. F. Cambridge Res. Lab., Bedford, Massachusetts. Rpt. No. AFCRL-63-62. INVESTIGATION OF CARRIER INJECTION ELECTRO-LUMINESCENCE. Semiann. Scient. rpt. No. 3, Feb. '63, 34 p. incl. tables, illus. and 10 ref.

Unclassified Report

The following advances in the growth of crystals of II-VI compounds (ZnSe and ZnTe) and in preparing electroluminescent junctions are related: A magnetic Czochralski puller for temperatures where magnets normally lose their susceptibility has been constructed. Experiences with the epitaxial growth of ZnSe and ZnTe are described. N-type ZnSe crystals exhibit light absorption due to free carriers. Electroluminescent emission at non-ohmic contacts is due to impact-ionization excitation. The new concept of tunnel-injection electroluminescence has been reduced to practice; light emission from CdS layers has bee.: obtained. A new effect, electrical modulation of photoluminescence in CdS, has been discovered. The compounds AlP and BP are apparently not miscible. The value for the lattice constant of AlP has been corrected. Injection electroluminescence was observed in boron phosphide crystals.

The methods for evaporation of ZnSe films on hot substrates were improved, and the light scattering and luminescent properties of such films were studied.

1. Injection Electroluminescence
2. Crystal Growth
3. Wide-Bandgap Semiconductors

I. AFCRL Project 4608, Task 460804
II. Contract AF19(604)8018
III. Radio Corp. of America, RCA Laboratories, Princeton, N. J.
IV. A. G. Fischer, W. H. Fonger, and A. S. Mason
V. Semiann. Scient. Rpt. No. 3
VI. In ASTIA collection
VII. Aval fr OTS

Electronic Research Directorate, A. F. Cambridge Res. Lab., Bedford, Massachusetts. Rpt. No. AFCRL-63-62. INVESTIGATION OF CARRIER INJECTION ELECTRO-LUMINESCENCE. Semiann. Scient. rpt. No. 3, Feb. '63, 34 p. incl. tables, illus. and 10 ref.

Unclassified Report

The following advances in the growth of crystals of II-VI compounds (ZnSe and ZnTe) and in preparing electroluminescent junctions are related: A magnetic Czochralski puller for temperatures where magnets normally lose their susceptibility has been constructed. Experiences with the epitaxial growth of ZnSe and ZnTe are described. N-type ZnSe crystals exhibit light absorption due to free carriers. Electroluminescent emission at non-ohmic contacts is due to impact-ionization excitation. The new concept of tunnel-injection electroluminescence has been reduced to practice; light emission from CdS layers has been obtained. A new effect, electrical modulation of photoluminescence in CdS, has been discovered. The compounds AlP and BP are apparently not miscible. The value for the lattice constant of AlP has been corrected. Injection electroluminescence was observed in boron phosphide crystals.

The methods for evaporation of ZnSe films on hot substrates were improved, and the light scattering and luminescent properties of such films were studied.

1. Injection Electro. luminescence
2. Crystal Growth
3. Wide-Bandgap Semiconductors

I. AFCRL Project 4608, Task 460804
II. Contract AF19(604)8018
III. Radio Corp. of America, RCA Laboratories, Princeton, N. J.
IV. A. G. Fischer, W. H. Fonger, and A. S. Mason
V. Semiann. Scient. Rpt. No. 3
VI. In ASTIA collection
VII. Aval fr OTS